

PAPER • OPEN ACCESS

## First-principles supercell calculations of small polarons with proper account for long-range polarization effects

To cite this article: Sebastian Kokott *et al* 2018 *New J. Phys.* **20** 033023

View the [article online](#) for updates and enhancements.

### Related content

- [First-principles determination of defect energy levels through hybrid density functionals and GW](#)  
Wei Chen and Alfredo Pasquarello
- [Issues in first-principles calculations for defects in semiconductors and oxides](#)  
Risto M Nieminen
- [Modelling of electron and hole trapping in oxides](#)  
A L Shluger, K P McKenna, P V Sushko et al.



## PAPER

## First-principles supercell calculations of small polarons with proper account for long-range polarization effects

## OPEN ACCESS

## RECEIVED

10 October 2017

## REVISED

18 January 2018

## ACCEPTED FOR PUBLICATION


14 February 2018

## PUBLISHED

28 March 2018

Original content from this work may be used under the terms of the [Creative Commons Attribution 3.0 licence](#).

Any further distribution of this work must maintain attribution to the author(s) and the title of the work, journal citation and DOI.

Sebastian Kokott<sup>1</sup> , Sergey V Levchenko<sup>1,2</sup>, Patrick Rinke<sup>3</sup> and Matthias Scheffler<sup>1,4</sup><sup>1</sup> Fritz Haber Institute of the Max Planck Society, Faradayweg 4-6, D-14195 Berlin, Germany<sup>2</sup> Laboratory of Modelling and Development of New Materials, NUST MISIS, Leninskiy prospekt 4, Moscow 119049, Russia<sup>3</sup> COMP/Department of Applied Physics, Aalto University School of Science, PO Box 11100, FI-00076 Aalto, Finland<sup>4</sup> University of California at Santa Barbara, CA 93106, United States of AmericaE-mail: [kokott@fhi-berlin.mpg.de](mailto:kokott@fhi-berlin.mpg.de)**Keywords:** density functional theory, polarons, finite-size corrections, electron–phonon couplingSupplementary material for this article is available [online](#)

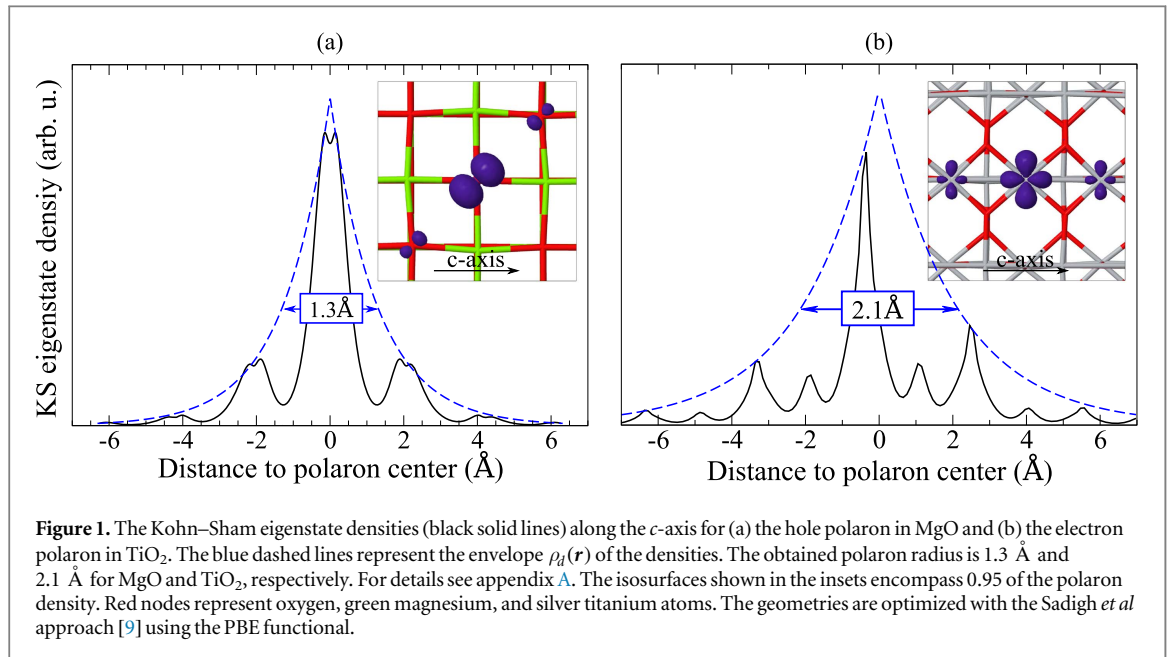
### Abstract

We present a density functional theory (DFT) based supercell approach for modeling small polarons with proper account for the long-range elastic response of the material. Our analysis of the supercell dependence of the polaron properties (e.g., atomic structure, binding energy, and the polaron level) reveals long-range electrostatic effects and the electron–phonon (el–ph) interaction as the two main contributors. We develop a correction scheme for DFT polaron calculations that significantly reduces the dependence of polaron properties on the DFT exchange–correlation functional and the size of the supercell in the limit of strong el–ph coupling. Using our correction approach, we present accurate all-electron full-potential DFT results for small polarons in rocksalt MgO and rutile TiO<sub>2</sub>.

## 1. Introduction

The electron–phonon (el–ph) interaction is fundamental to materials. It mediates, for example, the excitation of phonons in response to electronic excitations, which is especially pronounced in polar materials. These phonon excitations can stabilize a lattice distortion around a single excess charge (electron or hole). The excess charge and its accompanying lattice distortion are then referred to as a quasiparticle or more specifically as polaron. The formation and migration of polarons determine the properties of functional materials, such as their catalytic [1, 2] and photovoltaic [3] behavior. The direct observation of polarons in experiments, e.g. with electron-paramagnetic resonance [4], UV/IR spectroscopy [5], or scanning tunneling microscopy or spectroscopy [6] is difficult, and computational studies are required to interpret the experimental data correctly. In this work, we develop a new method that addresses challenges faced in computational modeling of small polarons in materials with strong el–ph coupling, in particular in oxides, with density functional theory (DFT).

Polarons can be classified by their size as quantified by the extent of their total wave function (electrons and ions). Large polarons are delocalized over several unit cells and usually appear, if the el–ph interaction is weak. Such polarons were first investigated by Fröhlich [7], who identified the Fröhlich coupling constant  $\alpha_{\text{Fröhlich}}$  [7] as good indicator for the el–ph interaction strength. In contrast, small polarons are mainly localized on one atomic site and form when the el–ph interaction is strong. Intermediate polarons [5] cover the size range in between. Pioneering work on small polarons was performed by Holstein [8], but taking only short-range interactions into account. Oxides fall into the intermediate to strong coupling regime, i.e.,  $\alpha_{\text{Fröhlich}} > 1$ . For instance, for MgO  $\alpha_{\text{Fröhlich}}$  is 4.4 and for rutile TiO<sub>2</sub> 2.2. We therefore expect small polaron formation in both of these oxides. However, since MgO and TiO<sub>2</sub> are strongly ionic, the distortion of the ionic lattice can be long-ranged in violation of the polaron classification scheme. Such polarons in which the excess charge is localized, but the lattice distortion effects long-ranged, are referred to as small Fröhlich polarons. Figure 1 illustrates the strong localization of the hole polaron in MgO and electron polaron in TiO<sub>2</sub>, obtained using the DFT approach described below.



To describe small Fröhlich polarons accurately in computational materials modeling, both long- and short-range interactions have to be treated appropriately. How to accomplish this task in DFT calculations that employ supercells, whose extent is typically smaller than the ionic lattice distortions, is the subject of this paper. Since small polarons can be regarded as a special type of a point defect, our study is also useful for point defect calculations of this type, which have so far eluded a reliable theoretical treatment.

The paper is structured as follows. In section 2 we derive the electrostatic and the el–ph contributions to the elastic long-range response of a material to a localized excess charge. We will then use this derivation to develop a correction scheme that removes artificial interactions from the supercell approach to obtain polaron properties in the dilute limit. In light of our new understanding, we analyze shortcomings of previous polaron approaches in section 3. In section 4, we demonstrate the efficiency of our approach for hole polarons in MgO and electron polarons in rutile TiO<sub>2</sub>.

## 2. Elastic long-range behavior

DFT in combination with the supercell approach has become the method of choice for the *ab initio* calculation of point defects in solids. However, the supercell approach suffers from finite-size effects, especially for charged defects. These finite-size effects include the interaction of the excess charge with its periodic images, with the compensating constant background charge introduced to keep the unit cell neutral, and with the periodic constraint on the atomic relaxation. To overcome these finite-size limitations, two strategies are commonly used: (a) extending the supercell and extrapolating to the dilute limit based on a scaling law, or (b) applying an *a posteriori* correction. For (a) only general knowledge about the size dependence is necessary. For example, the formation energy of a charged defect in the bulk as a function of the supercell size  $L$  ( $L = \Omega^{1/3}$ , where  $\Omega$  is the supercell volume) can be written as an inverse powerlaw:

$$E(L) = E(\infty) + a_1 \frac{1}{L} + a_3 \frac{1}{L^3}, \quad (1)$$

where  $E(\infty)$  is the formation energy in the dilute limit. This scaling law was derived by Makov and Payne [10]. The disadvantage of this procedure is that at least three supercell calculations of increasing size are needed to fit  $E(\infty)$  in equation (1), which is computationally very demanding, especially if atomic relaxations are included<sup>5</sup>.

Conversely, approach (b) requires an appropriate physical model for the long-range interactions in the solid. If only the electronic response to the excess charge is considered, its long-range contribution to the energy is described by a term proportional to  $1/\epsilon_{\infty}r$  (e.g. [12]). However, if the ionic response cannot be neglected, the problem becomes challenging, and so far this case has not been solved. It has been suggested that the long-range elastic contribution is similar to the electronic one, but with the high-frequency dielectric constant  $\epsilon_{\infty}$  replaced by the static one  $\epsilon_0$ , i.e., the long-range potential behaves classically like  $1/\epsilon_0r$ . However, corrections based on

<sup>5</sup> Alternatively, it is possible to embed the central region in the pristine crystal via a Green’s function approach (see e.g. [11]).

this assumption generally overestimate  $E(\infty)$ , especially for vacancies. This overestimation has two reasons. First, the aforementioned long-range behavior is a crude approximation, neglecting all details of the underlying phonon structure. Second, short-range screening can be much more efficient due to the strong coupling of the excess charge to localized phonon modes close to the defect. As a result, long-range screening will be different from  $\sim 1/\epsilon_0 r$ . The approach we present here for modeling polarons is therefore not directly applicable to defects that induce strong lattice distortions (e.g. vacancies). The modeling of such defects will be addressed in a subsequent publication. In the following we analyze the screening effects for the small polaron in detail and show that only in the strong-coupling limit of the el-ph interaction the substitution of  $\epsilon_\infty$  with  $\epsilon_0$  is a good approximation.

We start by splitting the long-range elastic potential<sup>6</sup>  $V^{\text{lr}}$  into the el-ph interaction  $V_{\text{el-ph}}^{\text{lr}}$  and electrostatic potential  $V_{\text{el-st}}^{\text{lr}}$ :

$$V^{\text{lr}} = V_{\text{el-st}}^{\text{lr}} + V_{\text{el-ph}}^{\text{lr}} \quad (2)$$

$V_{\text{el-st}}^{\text{lr}}$  is generated by the charge density  $\rho_d(\mathbf{r})$  of the localized excess charge. The Fourier transform of  $V_{\text{el-st}}^{\text{lr}}$  is then given by:

$$V_{\text{el-st}}^{\text{lr}}(\mathbf{k}) = 2\pi \frac{\rho_d(\mathbf{k})}{\mathbf{k}^T \epsilon_\infty \mathbf{k}}, \quad (3)$$

where  $\rho_d(\mathbf{k})$  is the Fourier transform of  $\rho_d(\mathbf{r})$ .

To obtain a corresponding expression for  $V^{\text{el-ph}}$  we first have to introduce additional assumptions. First, we will focus on ionic crystals. Second, we only consider the interaction of an electron with a single phonon at a time, neglecting higher-order contributions. Third, we assume that the adiabatic approximation (factorization of the electron and phonon wave functions) and strong el-ph coupling limit ( $\alpha_{\text{Fröhlich}} \gtrsim 4$ ) are applicable. With these assumptions the long-range part of  $V^{\text{el-ph}}$  reduces to [13]:

$$V_{\text{el-ph}}^{\text{lr}}(\mathbf{k}) = -\sum_{\nu} \frac{1}{\hbar \omega_{\mathbf{k}\nu}} |g_{\text{el-ph}}^{\text{lr}}(\mathbf{k}\nu)|^2 \rho_d(\mathbf{k}). \quad (4)$$

The potential in equation (4) is attractive, lending further stabilization to the polaron. An analytic expression for  $g_{\text{el-ph}}^{\text{lr}}$ , the el-ph matrix elements, was recently derived by Verdi and Guistino[14]:

$$g_{\text{el-ph}}^{\text{lr}}(\mathbf{k}\nu) = i4\pi e \sum_{\kappa} \left( \frac{\hbar}{2NM_{\kappa}\omega_{\mathbf{k}\nu}} \right)^{1/2} \frac{\mathbf{k}^T \mathbf{Z}_{\kappa}^* \mathbf{e}_{\mathbf{k}\nu}(\mathbf{k})}{\mathbf{k}^T \epsilon_\infty \mathbf{k}}, \quad (5)$$

where  $\nu$  labels the phonon mode,  $\omega_{\mathbf{k}\nu}$  is the corresponding phonon frequency of ion  $\kappa$  with mass  $M_{\kappa}$ ,  $\mathbf{Z}_{\kappa}^*$  is the Born effective charge tensor and  $\mathbf{e}_{\mathbf{k}\nu}(\mathbf{k})$  are the phonon eigenvectors of the dynamical matrix.

Equations (4) and (5) describe the scattering of all phonon modes with  $\rho_d$ . Thus, the long-range behavior of the el-ph interaction depends on the phonon structure across the entire phonon Brillouin zone, and the elastic behavior is not captured by the classical  $1/\epsilon_0 r$  limit. If we only consider the interaction of  $\rho_d$  with a single dispersion-less longitudinal-optical mode  $\omega_{\text{LO}}$ , we recover the limit of the Fröhlich el-ph interaction in the strong-coupling limit. With the Fröhlich matrix element (for the anisotropic case we refer to [15]):

$$g^F(k) = ie \left[ 2\pi \hbar \omega_{\text{LO}} \left( \frac{1}{\mathbf{k}^T \epsilon_\infty \mathbf{k}} - \frac{1}{\mathbf{k}^T \epsilon_0 \mathbf{k}} \right) \right]^{1/2} \quad (6)$$

we obtain the potential:

$$V_{\text{el-ph}}^{\text{lr}}(\mathbf{k}) = -2\pi \frac{\rho_d(\mathbf{k})}{\mathbf{k}^T \epsilon_\infty \mathbf{k}} + 2\pi \frac{\rho_d(\mathbf{k})}{\mathbf{k}^T \epsilon_0 \mathbf{k}}. \quad (7)$$

A similar expression for the electron-lattice interaction potential was previously derived by Pekar [16], assuming that the lattice polarization can be described classically. Upon substituting equations (7) and (3) into (2), we finally arrive at the classical limit of a screened potential for a localized charged distribution in an anisotropic medium:

$$V^{\text{lr}}(\mathbf{k}) = 2\pi \frac{\rho_d(\mathbf{k})}{\mathbf{k}^T \epsilon_0 \mathbf{k}}. \quad (8)$$

The el-ph potential given by equation (7) is an upper bound and, consequently, equation (8) is also an upper bound. This explains why any correction based on equation (8) overestimates the actual limit. We find that, despite the approximations we made,  $V^{\text{lr}}(\mathbf{k})$  in equation (8) is still appropriate for polarons in the intermediate coupling regime ( $1 \lesssim \alpha_{\text{Fröhlich}} \lesssim 4$ ). Vice versa, our derivation illustrates ways to improve the long-range model for polarons and charged point defects, if needed, since all assumptions are clearly defined.

<sup>6</sup> In this work by elastic potential we mean the sum of the Hartree potential of the excess charge and the potential from the ionic response to this charge.

Based on the knowledge of the long-range behavior, the errors due to finite size of the supercell can be corrected using *a posteriori* methods, such as the method of Freysoldt *et al* [12]. For technical details we refer to [12, 17]. Generalizing the Freysoldt method to an arbitrary interaction potential  $V(\mathbf{r})$  and anisotropic media (in the standard approach of Freysoldt *et al*,  $V(\mathbf{r}) = 1/\epsilon_\infty r$ ), the correction for the interaction energy is obtained as the difference between the energy of the artificial lattice of charged defects,  $E_{\text{latt}}$ , and the energy of an isolated defect,  $E_{\text{iso}}$ :

$$E_{\text{corr}}(\Omega) = E_{\text{latt}}(\Omega) - E_{\text{iso}} = \frac{1}{\Omega} \sum_{\mathbf{G} \neq 0} V(\mathbf{G}) q_d(\mathbf{G}) - \frac{1}{(2\pi)^3} \int V(\mathbf{k}) q_d(\mathbf{k}) d\mathbf{k}, \quad (9)$$

where  $V$  can be  $V_{\text{el-ph}}^{\text{lr}}$ ,  $V_{\text{el-st}}^{\text{lr}}$  or the sum of both, and  $q_d(\mathbf{k})$  is the Fourier transform of the excess charge distribution, and  $q$  is the total charge. A summary of the Freysoldt *et al* correction scheme including the meaning of the alignment terms  $q\Delta V$  can be found in the appendix C. Taking into account  $q\Delta V$ , the corrected energy is obtained as:

$$E(\infty) = E(\Omega) - E_{\text{corr}}(\Omega) + q\Delta V. \quad (10)$$

Having derived the correction for the elastic contribution, we can apply it to the polaron problem and investigate the effects of the two parts in equation (2) separately.

### 3. The polaron in a supercell

#### 3.1. The charged supercell

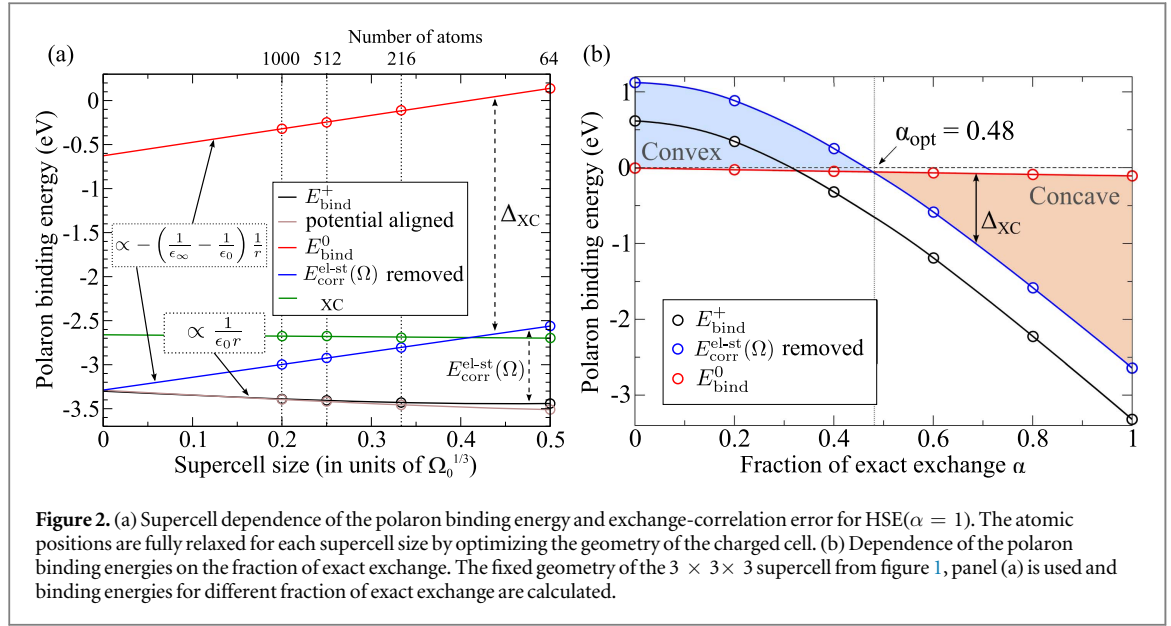
An important property of a polaron is its binding energy

$$E_{\text{bind}}^\pm = E^{\text{polaron}}(N \mp 1) - E^{\text{perf}}(N \mp 1), \quad (11)$$

where the energies have not been corrected for finite-size effects, yet. The plus in  $E_{\text{bind}}^\pm$  corresponds to electron removal (hole polaron), while the minus sign corresponds to electron addition (electron polaron).  $E^{\text{polaron}}$  is the total energy of the distorted system (polaron geometry),  $E^{\text{perf}}$  the total energy of the undistorted system. The number of electrons in the system are given in parenthesis, with  $N$  corresponding always to the neutral system. A negative  $E_{\text{bind}}^\pm$  indicates an energy gain and a stable (self-trapped) polaron.

In the following we focus on the hole polaron for brevity, since only small adjustments of the formalism are needed for the electron polaron case. The simplest way to calculate the polaron binding energy is straightforward: in equation (11)  $E^{\text{polaron}}(N \mp 1)$  is computed with DFT and full structure relaxation in the charged supercell. To ease the system out of possible high symmetry configurations an initial symmetry-breaking distortion might have to be applied. Finite-size effects are expected to be small, since the elastic long-range interaction falls off with  $1/\epsilon_0 r$  and the static dielectric constant  $\epsilon_0$  is usually large ( $\gtrsim 10$ ) for ionic crystals (however, as demonstrated and explained below, the dependence of the polaron binding energy defined by equation (11) on the approximations in the exchange-correlation functional is strong). The supercell dependence of  $E_{\text{bind}}^+$  for MgO is shown in figure 2, panel (a), where we used HSE06 hybrid functional [18, 19] with the fraction of exact exchange  $\alpha = 1$  (denoted HSE06( $\alpha = 1$ ); see section 4 for more computational details). We find a small hole polaron mainly localized at the central oxygen atom. The displacements of the nearest neighbors are of the order of 0.1 Å and decaying fast away from the center. The shape of the excess charge density distribution is *p*-like. For sufficiently large supercells, when the long-range regime is valid, the dependence of the binding energy on the supercell size  $L$  becomes  $1/\epsilon_0 L$ . From the slope of  $E_{\text{bind}}^+(1/L)$  at  $1/L = 0$  we obtain  $\epsilon_0 = 10.32$ , in good agreement with the experimental static dielectric constant for MgO  $\epsilon_0 = 9.8$ .

Next, we calculate the correction for the artificial electrostatic interaction due to the periodic arrangement of the holes and their interaction with the constant background, using equation (9) with the potential  $1/\epsilon_\infty r$ . To model the excess charge density  $\rho_d(\mathbf{r})$  needed here and for following finite-size corrections, we fit the envelope of the KS eigenstate density (decays exponentially for a localized state) with an exponential function  $\rho_{\text{model}} = A \exp(-|r - r_0|/\gamma)$ , where  $A$  is a normalization constant,  $r_0$  is the center of the polaron, and  $\gamma$  the fitting parameter corresponding to the polaron radius (see appendix A). Additionally, we calculated the alignment term  $\Delta V$  in equation (10) between the charged, neutral, and model (i.e., including the model excess charge density compensated by a constant background charge) systems following the approach outlined in [17]. After this correction, according to equation (2) the remaining contribution is due to the long-range el-ph interaction. This contribution is shown by the blue line in figure 2, panel (a). The line is almost perfectly



straight, and the slope is equal to  $\epsilon_{\infty}^{-1} - \epsilon_0^{-1} = 0.32$ , where  $\epsilon_0 = 10.32$  is taken from the fit of  $E_{\text{bind}}^+$  presented above, and  $\epsilon_{\infty} = 2.4$  is obtained from an independent calculation<sup>7</sup>. This analysis explains the role of different long-range interactions in equation (2) in the supercell dependence of polaron properties.

Thus, the approximations in equation (7) work well for MgO, which is expected since it has only one longitudinal optical phonon mode, strong el-ph coupling, and is an isotropic material. However, we find that the polaron binding energy defined by equation (11) is extremely sensitive to the approximations in the exchange-correlation functional. Figure 2, panel (b), shows the dependence of the binding energy on the fraction of exact exchange  $\alpha$  in the HSE06 functional. Within a small range  $\pm 0.05$  of  $\alpha$  around the standard value (0.25) the binding energy changes by about 0.5 eV. This leads to a qualitative change in small polaron stability, from a stable self-trapped polaron (negative binding energy) to an unstable small polaron (positive binding energy). This strong functional dependence makes even a qualitative assessment of the existence of a self-trapped polarons impossible. Several approaches have been suggested in the literature for determining the correct or at least optimal value of  $\alpha$  [20–26]. Here we focus on *restoring the IP theorem* [22] as a consistent *DFT-based* solution of the problem.

In (exact) DFT within the scope of Kohn–Sham (KS) scheme the vertical ionization potential IP should be equal to the negative of the highest occupied KS state energy  $\epsilon_{\text{ho}}$  in the system:

$$\text{IP} = E(N - 1) - E(N) = -\epsilon_{\text{ho}}(N), \quad (12)$$

where  $E(N - 1)$  and  $E(N)$  are total energies of the ionized and neutral system, respectively. In this work we refer to this relation as IP theorem, but it is also known as HOMO-I condition [20] or Generalized Koopmans' theorem [22], and is directly related to the straight-line dependence of the total energy on occupation of the highest-occupied state [27] or the fact that the position of  $\epsilon_{\text{ho}}$  is independent on its occupation. Equation (12) is always correct for any extended (delocalized) state, as was already pointed out by Janak (1978) and extended to the case of the generalized KS scheme by Perdew *et al* [28]. However, for a given density functional approximation (DFA) equation (12) does not necessarily hold, if the orbital is localized, unless the satisfaction of the straight-line condition is explicitly included in the design of the functional. The deviation from the straight line  $\Delta_{\text{XC}}(\alpha)$  is described by two contributions to equation (12):

$$E(N - 1) - E(N) = -\epsilon_{\text{ho}}(N) + \Delta_{\text{XC}}(\alpha), \quad \Delta_{\text{XC}} = \Pi + \Sigma, \quad (13)$$

with the self-interaction error  $\Pi$  causing a convex curvature of the total energy as a function of occupation, and the orbital relaxation  $\Sigma$  a concave curvature. The optimal  $\alpha = \alpha_{\text{opt}}$  minimizing the XC error [21, 29] is then determined from the condition  $\Delta_{\text{XC}}(\alpha_{\text{opt}}) = 0$ .

The IP theorem (equation (12)) was originally proven for finite systems, and transferring it to a solid with periodic boundary conditions needs special care. For any finite supercell with volume  $\Omega$  the energy of the artificial electrostatic interactions due to the periodic arrangement ( $E_{\text{corr}}^{\text{el-st}}(\Omega)$ ), obtained using equation (9) with potential from equation (3) has to be removed from  $E(N - 1)$ :

<sup>7</sup> The dielectric constant  $\epsilon_{\infty}$  was obtained by fitting the formation energy with equation (1) for the unrelaxed doubly charged oxygen vacancy in MgO for three different supercell sizes.

$$E(N-1) - E_{\text{corr}}^{\text{el-st}}(\Omega) - E(N) = -\varepsilon_{\text{ho}}(N) + \Delta_{\text{XC}}(\alpha), \quad (14)$$

since it would only vanish in the limit of an infinite supercell. Combining equations (14) and (11), we get:

$$E_{\text{bind}}^+ = E_{\text{bind}}^0 + E_{\text{corr}}^{\text{el-st}} + \Delta_{\text{XC}}(\alpha), \quad (15)$$

where  $E_{\text{corr}}^{\text{el-st}}$  stands for the artificial electrostatic interaction energy for the distorted geometry, since for the perfect geometry it is zero. The quantity

$$E_{\text{bind}}^0 = \Delta E^{\text{polaron}} - E_0 \quad (16)$$

is calculated using only *neutral* unit cells, with the energy of distortion from perfect to polaronic geometry  $\Delta E^{\text{polaron}} = E^{\text{polaron}}(N) - E^{\text{perf}}(N)$  and the polaron level energy with respect to the VBM  $E_0 = \varepsilon_{\text{ho}}^{\text{polaron}}(N) - \varepsilon_{\text{VBM}}^{\text{perf}}(N)$ . According to equation (15), when  $\Delta_{\text{XC}}(\alpha)$  is zero,  $E_{\text{bind}}^0$  represents the polaron binding energy corrected for the artificial electrostatic interaction.

The use of equation (14) to determine the optimal fraction of exact exchange  $\alpha_{\text{opt}}$  implies a fixed external potential of nuclei. However, the IP theorem is expected to be valid for a range of ionic displacements, as long as the leading orbital character of the adiabatic ground state does not change. This is the case for the polaronic state, whose character is tied to the character of the corresponding band edge. The fact that  $\Delta_{\text{XC}}$  is independent of the supercell size (see figure 2(a)) supports this hypothesis, since  $\Delta_{\text{XC}}$  would be sensitive to changes in the shape.

$E_{\text{bind}}^0$  is shown in figure 2, panel (a), as red line (top-most line), where the optimized polaron geometry of the charged supercell is used. Note that, despite including only quantities calculated using neutral unit cells,  $E_{\text{bind}}^0$  has a strong dependence on the unit cell size. As discussed below, this dependence is due to the interaction of the ionic relaxations in different unit cells. Taking the difference between the blue and the red lines, we find that the exchange-correlation error  $\Delta_{\text{XC}}$  is practically independent on the unit cell size (green line in figure 2, panel (a)), starting from the smallest supercell with 64 atoms we have considered. This implies that  $\Delta_{\text{XC}}(\alpha)$  in equation (14) could be calculated even in the smallest supercell in order to estimate  $\alpha = \alpha_{\text{opt}}$  and then reused for any larger supercell. For obtaining the optimized  $\alpha = \alpha_{\text{opt}}$  we have to remove  $E_{\text{el-st}}(\Omega)$  from the binding energy  $E_{\text{bind}}^+$  and determine the intersection with  $E_{\text{bind}}^0$ . The result is shown in figure 2, panel (b), and we obtain  $\alpha_{\text{opt}} = 0.48$ . Since the dependence on  $\alpha$  is not linear, at least three different values of  $\alpha$  have to be calculated to estimate  $\alpha_{\text{opt}}$ . Additionally for each value of  $\alpha$  the dielectric constant  $\epsilon_{\infty}$  has to be calculated. Thus, the simulation of the polaron in a charged supercell is computationally demanding, since it is extremely sensitive to the underlying functional. In the next subsection we demonstrate an approach to overcome this problem.

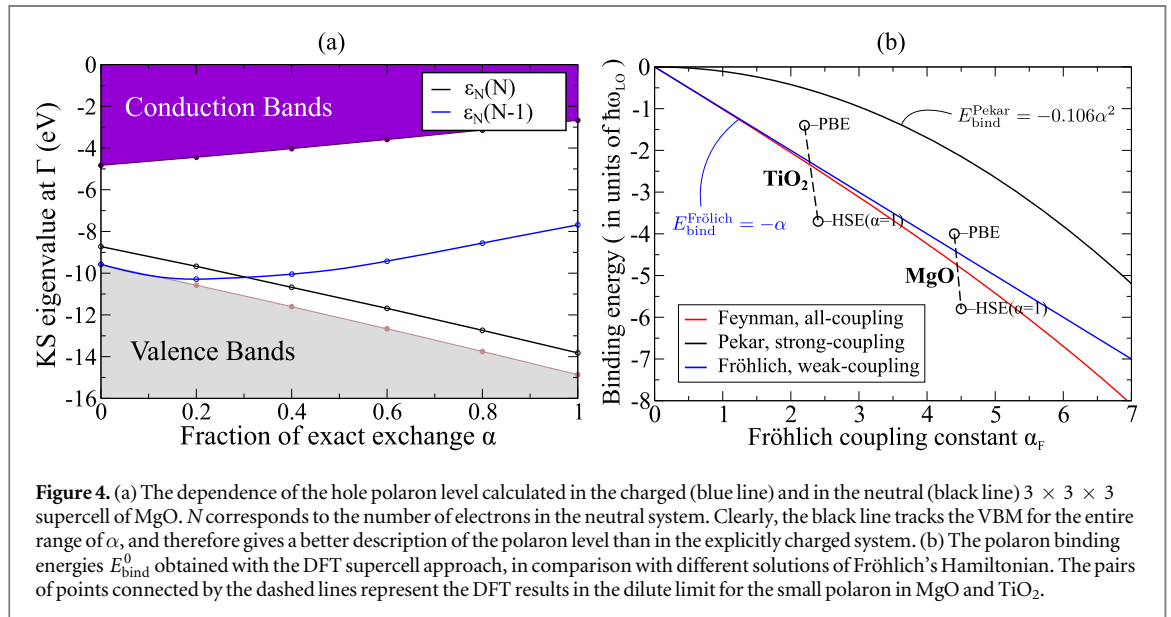
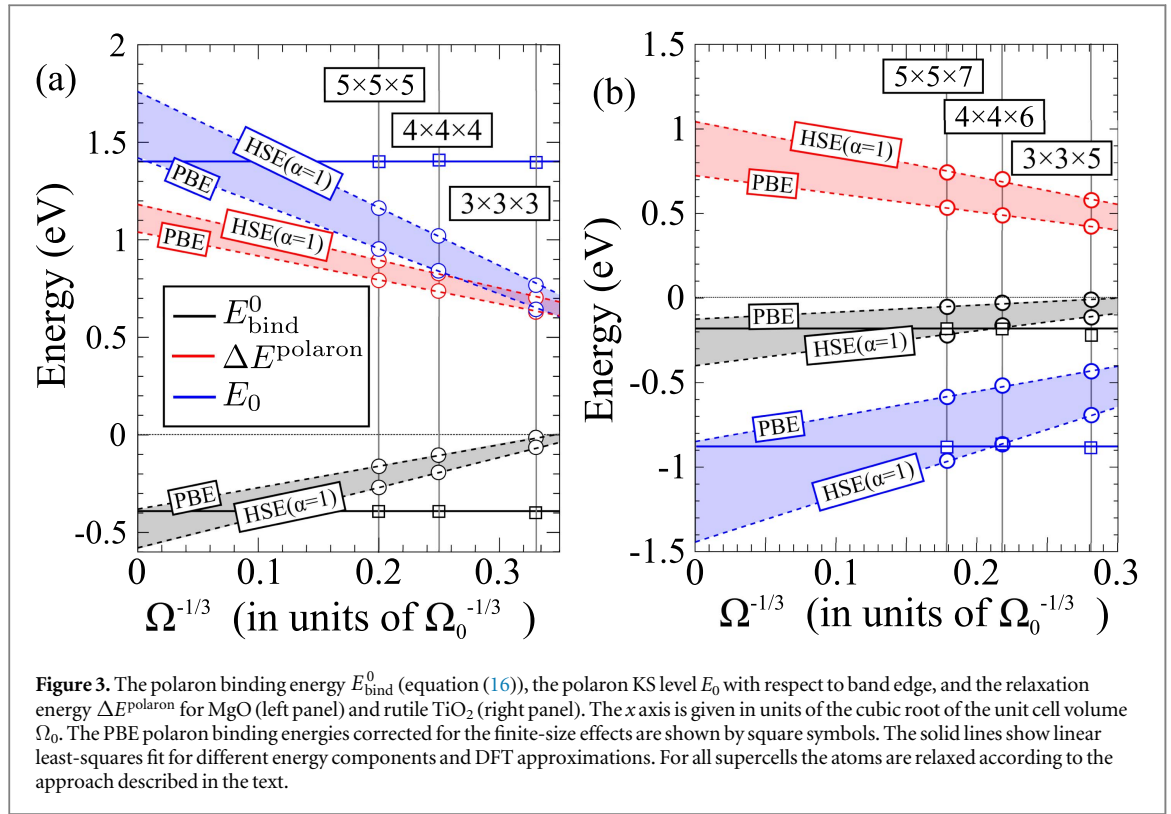
### 3.2. The neutral supercell

As mentioned above,  $E_{\text{bind}}^0$  in equation (15) is equal to the polaron binding energy corrected for the artificial electrostatic interaction, only when  $\Delta_{\text{XC}}(\alpha)$  vanishes. However, similar to previous work [9, 30] we find that  $E_{\text{bind}}^0$  is far less sensitive to the underlying functional than  $E_{\text{bind}}^+$ , as can be seen for MgO in figure 2, panel (b). The same is true for  $\text{TiO}_2$ , but the remaining dependence is larger than for MgO (see figure 3). This has an interesting implication:  $E_{\text{bind}}^0$  is the polaron binding energy with most of the exchange-correlation error removed. The reason for the insensitivity of  $E_{\text{bind}}^0$  on the functional remains unclear [9], but it seems to benefit from the character of the closed electron shells.

As a consequence, even with PBE we find a stable self-trapped hole polaron in MgO, which is not the case when charged supercells are used. Also, we find that the polaron level with respect to the band edge ( $E_0$ ), calculated using a neutral supercell, is insensitive to the functional, as can be seen in figure 4(a). A stronger functional dependence of  $E_0$  is expected when the character of the polaronic state or states of the band edges are sensitive to the functional.

Using  $E_{\text{bind}}^0$  for calculating polaron binding energies has been first implicitly introduced by Zawadski *et al* [30]. The independence of  $E_{\text{bind}}^0$  on the functional has been discussed by Sadigh *et al* [9]. In their work, Sadigh *et al* have also suggested a way to obtain forces for a polaronic distortion directly using  $E_{\text{bind}}^0$  potential-energy surface (PES). This facilitates the calculation of accurate elastic response to the excess charge at the level of a hybrid functional, but at the cost of a PBE calculation.

Thus, using the  $E_{\text{bind}}^0$  PES instead of charged supercells allows us to significantly reduce the functional dependence. Naively, one may expect that the supercell dependence is also reduced, since only neutral supercell calculations are performed. However, this is not the case. As can be seen from figure 2, panel (a), the dependence of  $E_{\text{bind}}^0$  on the supercell size is much stronger than in the case of charged supercells. This dependence is due to the artificial interaction between ionic relaxation fields in different supercells. Indeed, the  $E_{\text{bind}}^+ - E_{\text{corr}}^{\text{el-st}}$  and  $E_{\text{bind}}^0$  supercell dependence are practically identical and correspond to the long-range part of the el-ph interaction potential given by equation (7) in the strong el-ph coupling limit. This understanding allows us to introduce an *a posteriori* correction  $E_{\text{corr}}^{\text{el-ph}}$  calculated using equation (9) with  $V = V_{\text{el-ph}}^{\text{lr}}$  of equation (7), which removes the dependence of  $E_{\text{bind}}^0$  on the supercell size. To remove the artificial interaction terms, we use the approach of Freysoldt *et al* [12, 17], but for a different long-range potential, namely the one given by



equation (7). This new correction scheme relies on the assumption of a strong el-ph coupling, but, as demonstrated below, works reasonably well also for intermediate coupling regimes.

The polaron level  $E_0$  also depends on the supercell size. Because of special properties of the small polaron in the adiabatic strong-coupling limit, it is possible to relate the polaron binding energy to the polaron level, in accordance with Pekar's 1:2:3:4 theorem [31]. It follows from the theorem that (see details in appendix B):

$$E_0(\infty) = E_0(\Omega) + 2 \cdot E_{\text{corr}}^{\text{el-ph}}(\Omega). \quad (17)$$

Thus, the correction to  $E_0(\Omega)$  in a finite supercell is expected to be about twice as large as for the polaron binding energy calculated using neutral supercells. Indeed, this is what we observe for MgO (see figure 3, panel (a)), where the absolute value of the  $E_0(L)$  slope is almost exactly twice of the absolute value of the  $E_{\text{bind}}^0$  slope. For TiO<sub>2</sub>, the relation between the  $E_0(L)$  and  $E_{\text{bind}}^0$  dependencies deviates from the one derived from Pekar's model (see figure 3, panel (b)) due to a weaker el-ph coupling, as discussed in detail in section 4.



In summary, we find that in this approach the dependence on the exchange-correlation approximation is drastically reduced, but the finite-size effects are significantly more pronounced. However, these effects, caused by the el-ph long-range potential (equation (7)), can be corrected using the approach of Freysoldt *et al*, but with the potential  $V_{\text{el-ph}}^{\text{lr}}$ . This makes possible using moderately sized supercells and semi-local functionals to predict polaron properties, as demonstrated in the next section.

#### 4. Polarons in rocksalt MgO and rutile TiO<sub>2</sub>

Building on the findings and understanding obtained in the previous sections, we formulate our approach for a reliable calculation of polaron properties:

- (i) We obtain the atomic structure of the polaron using the PBE functional (corresponding to HSE06( $\alpha = 0$ )), where the forces for the atomic relaxation being evaluated according to the approach of Sadigh *et al* [9].
- (ii) HSE06( $\alpha = 1$ ) calculations (as a limiting case) are performed for the fixed geometries obtained with PBE. This allows the estimation of the functional dependence for the systems.
- (iii) The polaron binding energies are calculated using equation (15). The finite-size correction for the binding energy is calculated using equation (9) with the potential from equation (7). The correction for the polaron level is calculated as twice the correction for the binding energy.

The different sign of the correction for the hole polaron versus the electron polaron (compare panels (a) and (b) in figure 3) is explained by the fact that the equation for the electron affinity has to be used for the electron instead of the ionization potential for the hole.

We use the hybrid-functional implementation [32] in the all-electron full-potential electronic-structure package FHI-aims [33–35]. The evaluation of forces and total energies are computed with FHI-aims using the default *light* settings, to obtain consistent results for all unit cell sizes. As is shown in the supplementary information (SI) is available online at [stacks.iop.org/NJP/20/033023/mmedia](https://stacks.iop.org/NJP/20/033023/mmedia), using default *tight* settings, which are the recommended settings for well-converged calculations, does not affect the results for the smallest supercell. As a demonstration, we apply our new approach to polarons in MgO and rutile TiO<sub>2</sub>. For the cubic 8-atom MgO unit cell we use a lattice constant of  $a = 4.211 \text{ \AA}$  obtained with HSE06 ( $\alpha = 0.25$ ), and a  $\Gamma$ -centered  $8 \times 8 \times 8$  k-grid. The number of k-points for each direction is scaled down linearly for larger supercell sizes. For the tetragonal 6-atom TiO<sub>2</sub> unit cell we use  $a = 4.64 \text{ \AA}$  and  $c = 2.97 \text{ \AA}$  obtained with the PBE functional and a  $9 \times 9 \times 15$  k-grid. Due to one more degree of freedom the positions of the atoms are optimized, too, using the PBE functional (for details see SI).

The results for a hole polaron in MgO and an electron polaron in rutile TiO<sub>2</sub> are shown in figure 3. For every supercell size we allow all atoms to relax to obtain the full elastic contribution within the cell. The corrected  $E_{\text{bind}}^0$  values for each supercell are shown for PBE. For the Freysoldt *et al* correction we used the radii obtained by fitting the KS eigenstate densities as it is demonstrated in figure 1 for the  $3 \times 3 \times 3$  MgO, panel (a) and  $3 \times 3 \times 5$  TiO<sub>2</sub> supercell, panel (b). The variation of the polaron radius is only small with the fraction of exact exchange (see SI) and is not affecting the contribution of the Freysoldt *et al* correction. Clearly, the supercell size dependence of  $E_{\text{bind}}^0$  for both MgO and TiO<sub>2</sub> agrees very well with the behavior corresponding to the el-ph long-range contribution described by equation (7). As mentioned above, the Frölich coupling constant  $\alpha_{\text{Frölich}}$  is equal to 4.4 for MgO and 2.2 for TiO<sub>2</sub>. Thus, MgO is better described by Pekar's potential equation (7), and the size-corrected binding energy practically coincides with the binding energy obtained from a linear extrapolation to the dilute limit. For TiO<sub>2</sub>, the corrected energy deviates (surprisingly only slightly) from the extrapolated one (within 0.05 eV), reflecting approximations in Pekar's model. Also, the functional dependence of the energies is stronger for TiO<sub>2</sub>, indicating a larger contribution of the short-range effects to the binding energy. Additionally, we observe that the atomic structure is sensitive to the functional as well demonstrating limitations of obtaining polaron atomic geometries with only the PBE functional, even on the PES corresponding to  $E_{\text{bind}}^0$ , which is much less sensitive to the approximations in the functional than the PES of a charged supercell. This sensitivity is connected to delocalization errors and missing static correlation originated in the d-orbitals. However, the changes in the geometry as a function of  $\alpha$  are still small, and we use the configurations of the perfect system obtained with PBE. We find final polaron binding energies in the dilute limit  $-0.38... - 0.58 \text{ eV}$  for MgO and  $-0.14... - 0.41 \text{ eV}$  for TiO<sub>2</sub>, where the range indicates changes in  $\alpha$  from 0 to 1. For the polaron level with respect to the band edge we find  $1.42... 1.74 \text{ eV}$  for MgO and  $-0.86... - 1.44 \text{ eV}$  for TiO<sub>2</sub>. These results remain both qualitatively and quantitatively consistent across a broad range of functionals generated by varying the fraction of exact exchange. This consistency is remarkable when compared to previous theoretical studies, especially for TiO<sub>2</sub>, since it was either shown that the small polaron formation is expected only for a certain range

of a parameter, e.g. for DFT+ $U$  [6, 36] or HSE( $\alpha$ ) [37], or it was demonstrated only for a specific value of a parameter, e.g. for HSE( $\alpha = 0.25$ ) [38]. Additionally, it is interesting to note that contrarily to anatase TiO<sub>2</sub> [39, 40] small electron polarons do form in rutile (see figure 1(b)). However, we could not find a stable small hole polaron in rutile.

One of the advantages of our DFT approach for calculating polaron properties over Fröhlich's Hamiltonian is that the ionic lattice is considered explicitly in our polaron model. Such a description is particularly appropriate for small polarons that are of interest here. The DFT approach is based on the adiabatic (Born–Oppenheimer) approximation. As such, in the strong-coupling limit, it physically corresponds to Pekar's polaron model, the adiabatic static description of polarons, where the polarization of the lattice is treated classically. Figure 4, panel (b) shows a comparison of the DFT results for MgO and TiO<sub>2</sub> with Pekar's model and other approximate solutions of Fröhlich's Hamiltonian. Pekar's model predicts smaller (in absolute values) polaron binding energies compared to DFT. Considering that in Pekar's model (as well as in Fröhlich's Hamiltonian) the electron (or hole) only interacts with a single phonon mode, it is not surprising that Pekar's solution only provides an upper limit to the polaron binding energy. The el–ph interaction for the small polaron includes couplings to almost all the phonon modes throughout the Brillouin zone, leading to a further stabilization of the polaron in our simulations. The DFT results are close to Feynman's approximate solution of the Fröhlich Hamiltonian [41]. However, Feynman's model includes quantum fluctuations and non-adiabatic effects [42], not accounted for in our DFT approach. Thus, on the one hand the comparison between Pekar's and Feynman's approximate solution shows the significance of possible non-adiabatic effects for polarons in oxides. On the other hand, by comparing Pekar's solution with our DFT results the importance of the proper microscopic treatment of the lattice polarization is illustrated.

To make a connection to experimentally accessible quantities, in particular photoluminescence (PL) measurements, accurately predicting the position of the polaron level is important. Since the quantities obtained with the neutral PES  $E_{\text{bind}}^0$  are weakly dependent on the underlying functional, the fraction of exact exchange  $\alpha$  can be used to tune the gap  $E_{\text{gap}}$  to recover the experimental band gap. The main PL peak due to the small polaron formation can be expected at:

$$PL = E_{\text{gap}} - |E_0|. \quad (18)$$

For MgO the experimental band gap was measured to 7.8–7.9 eV [43], which can be simulated by a fraction  $\alpha = 0.4$ . Based on our HSE06( $\alpha = 0.4$ ) calculations, the PL peak should be at  $6.3 \pm 0.1$  eV. Cathodoluminescence experiments [50] assign a peak at 6.9 eV to a self-trapped exciton, but is not clear whether the signal is due to excitons (or polarons) in the bulk or trapped at surface defects. For TiO<sub>2</sub> a fraction  $\alpha = 0.2$  is needed in order to reproduce the experimental band gap of 3.0 eV [44], and the corresponding PL peak is predicted to be at  $2.1 \pm 0.1$  eV. This is in good agreement with experimental findings of  $PL = 2.34$  eV for rutile powders [45] or direct measurements of the polaron level  $E_0 = 0.7 \pm 0.1$  eV with scanning tunneling spectroscopy [6]. It should be noted that the latter measurements likely refer to subsurface oxygen vacancies, and hence the agreement with our results may be fortuitous. We note that the results provided here only represent an upper limit for the polaron level or lower limit for the PL peak, since neither finite-temperature nor non-adiabatic effects are taken into account.

## 5. Conclusions

In this work, we developed a new approach for first-principles modeling of small polarons in materials using DFT supercell calculations. Because on the one hand, the standard charged supercell approach allows us to obtain polaron properties in the dilute limit (for moderately large finite supercells and values of  $\epsilon_0$  finite-size errors can be even neglected), but the results strongly depend on the underlying exchange–correlation functional. On the other hand, the approach of Sadigh *et al* [9] significantly reduces the dependence on the functional, but, as we demonstrate, introduces a strong dependence on the supercell size. We show that the large finite-size errors in the latter approach are due to constraints imposed on the elastic response to the excess charge by the periodic boundary conditions, and suggest a way to correct the errors for finite supercells. The correction relies on the validity of Pekar's model [16] for the long-range response, based on approximations corresponding to the adiabatic strong (in Fröhlich's sense) el–ph coupling limit. As a result, our approach allows us to obtain polaron properties in the dilute limit and at the same time reduce the exchange–correlation errors, so that even semi-local functionals can be used to reliably estimate polaron level, binding energy, and atomic structure. For more accurate modeling of polaron effects on PL in materials, the use of hybrid-density functionals or methods beyond DFT, such as the GW approach [46–48], is still necessary.

We apply the developed approach to small polarons in MgO and rutile TiO<sub>2</sub>. We find that the hole polaron in MgO indeed behaves as Pekar's polaron at the long-range, as expected based on the large value of Fröhlich's constant. For electron polarons in TiO<sub>2</sub>, our approach also works surprisingly well, considering the weaker el–

ph coupling in this material. Our all-electron full-potential results support the existence of a small electron polaron in rutile TiO<sub>2</sub> in agreement with previous work [6, 37].

## Acknowledgments

This work was supported by the DFG Excellence Cluster ‘UniCat’ and the Leibniz ScienceCampus ‘GraFOx’. SVL is grateful for the support by the Ministry of Education and Science of the Russian Federation in the framework of Increase Competitiveness Program of NUST ‘MISIS’ (No K2-2016-013) implemented by a governmental decree dated 16 March 2013, No 211.

## Appendix A. Pekar’s polaron and its relation to KS eigenstates

The objective of the appendix is to show how analytical polaron models are connected to the actual many-body problem treated with DFT. Especially, the relation of the polaron wave function to the highest occupied (ho) or lowest unoccupied (lu) KS state is discussed below.

Pekar’s polaron model [16] can be derived from the Fröhlich Hamiltonian [7] in the adiabatic static strong coupling limit, as was shown for example by Devreese [13] (see also citation in it for original works). In this limit, assuming adiabatic separation of ionic and electronic degrees of freedom, the el–ph interaction has the form:

$$V_{\text{el-ph}}(\mathbf{r}) = -\frac{1}{\kappa} \int \frac{|\Phi(\mathbf{r}')|^2}{|\mathbf{r} - \mathbf{r}'|} d^3r' \quad (\text{A.1})$$

which is the classical response of a polar dielectric to an extended charge distribution. The inverse dielectric constant  $\kappa^{-1} = \epsilon_{\infty}^{-1} - \epsilon_0^{-1}$  describes the polarization of the rigid ions in the medium by the electron or hole. For simplicity, here we assume an isotropic medium (the dielectric response is described by a single constant). Let us regard equation (A.1) as a perturbation of the perfect system  $H_{\text{perf}}$ —i.e. the single-electron Hamiltonian, where the electron has been placed at the bottom of the conduction band minimum (CBm)  $\phi_{\text{CBm}}$  with energy  $\epsilon_{\text{CBm}}$  of the non-interacting system (this is the scenario for the electron polaron):

$$H_{\text{perf}} \phi_{\text{CBm}} = \epsilon_{\text{CBm}} \phi_{\text{CBm}}. \quad (\text{A.2})$$

Following the Kohn–Luttinger perturbation theory [49] the solution of:

$$(H_{\text{perf}} + V_{\text{el-ph}})\Psi = E\Psi \quad (\text{A.3})$$

in first order is given by:

$$\begin{aligned} E &= \epsilon_{\text{CBm}} + E_0, \\ \Psi &= \phi_{\text{CBm}} \Phi, \end{aligned} \quad (\text{A.4})$$

where  $E_0$  and  $\Phi$  are obtained from the solution of the effective Hamiltonian of the charge with an effective mass  $m^*$  [49] (without taking into account polaronic effects):

$$\begin{aligned} (H_{\text{kin,eff}} + V_{\text{el-ph}})\Phi &= E_0\Phi, \\ \left( -\frac{\nabla^2}{2m^*} - \frac{1}{\kappa} \int \frac{|\Phi(\mathbf{r}')|^2}{|\mathbf{r} - \mathbf{r}'|} d^3r' \right) \Phi(\mathbf{r}) &= E_0\Phi(\mathbf{r}), \end{aligned} \quad (\text{A.5})$$

with the effective mass  $m^*$  from the CBm. With equation (A.5) we recover the original problem of Pekar’s polaron and  $E_0$  is the energy of the bound (polaron) state relative to the conduction-band edge for the case of an electron polaron.

Equation (A.5) does not contain microscopic details. However, it can be regarded as describing asymptotic el–ph interaction far away from the localized part of the excess electron charge distribution and, thus,  $\Phi(\mathbf{r})$  is the asymptotic solution of equation (A.5). According to equation (A.4),  $\Phi(\mathbf{r})$  represents the envelop of the original electronic state  $\phi_{\text{CBm}}$  and is expected to decay exponentially with distance. The electron KS eigenstate  $\phi_{\text{lu}}^{\text{DFT}}$  corresponding to  $\epsilon_{\text{lu}}(N)$  in the DFT calculation at the *distorted* (polaron) geometry is the polaron wave function  $\Psi$ . Thus, the envelop of  $\phi_{\text{lu}}^{\text{DFT}}$  shows the localization of  $\rho_d(\mathbf{r})$  needed for the correction scheme equation (9) in order to fit  $\rho_m(\mathbf{r})$ . An example of  $\rho_d(\mathbf{r})$  calculated with DFT and the fitted envelope  $\rho_m(\mathbf{r})$  is shown in figures 1(a) and (b) for MgO and TiO<sub>2</sub>, respectively.

## Appendix B. Pekar's 1:2:3:4 theorem

For arbitrary coupling constants in the Fröhlich Hamiltonian:

$$H_{\text{Fröhlich}} = H_{\text{kin,eff}} + H_{\text{ph}} + V_{\text{el-ph}}, \quad (\text{B.1})$$

with the Hamiltonian of the phonons  $H_{\text{ph}}$ , it has been shown [31] that there exist fixed ratios of the effective kinetic energy  $E_{\text{kin,eff}}$ , lattice distortion (phonon field) energy  $\Delta E^{\text{polaron}}$ , the polaron state energy  $E_0$ , and the el-ph interaction energy  $E_{\text{el-ph}}$ :

$$E_{\text{kin,eff}} : \Delta E^{\text{polaron}} : -E_0 : -E_{\text{el-ph}} = 1 : \eta(\alpha_{\text{F}}) : 3 : 4, \quad (\text{B.2})$$

where  $\eta$  depends on the value of Fröhlich coupling constant  $\alpha_{\text{F}}$ . In the limit of strong el-ph coupling ( $\alpha_{\text{F}} \rightarrow \infty$ ), the polaron energy is dictated by the polarization of the lattice, and  $\eta$  approaches 2. From this it follows:

$$E_{\text{bind}} = E_{\text{kin,eff}} + \Delta E^{\text{polaron}} + E_{\text{el-ph}} = E_{\text{kin,eff}} + \frac{1}{2}E_{\text{el-ph}}, \quad (\text{B.3})$$

$$E_0 = E_{\text{kin,eff}} + E_{\text{el-ph}}. \quad (\text{B.4})$$

Equations (B.3) and (B.4) clearly show the dependence of the binding energy and the polaron level on the energy of the el-ph interaction. The latter energy is the one that remains to be corrected for the artificial supercell interactions, and thus the correction for the polaron level has to be twice of the correction for the binding energy, which leads to equation (17).

However, these ratios equation (B.2) are only based on an effective single-particle model (equation (A.5)). In our microscopic (DFT) model, additional (short-range) contributions to the energy components and deviations of  $\eta \leq 2$  lead to violation of the above ratios. In particular for TiO<sub>2</sub> the ratios are not preserved. However, for MgO, where the Fröhlich constant is 4.4, indicating indeed a strong el-ph coupling, the ratios are close to the ones found by Pekar, and the polaron level and binding energies calculated from the model are close to the ones from DFT calculations, as described in the text.

## Appendix C. Freysoldt *et al* correction scheme for finite-size effects in a nutshell

A repeating point in this paper is the correction of finite-size effects for supercell calculations. For completeness we present the main ideas of the correction scheme proposed by Freysoldt *et al* [12, 17]. Starting point is the simulation of a charged point defect in an otherwise pristine crystal causing a localized excess-charge distribution  $\rho_d$ . It is assumed that for a sufficient large supercell the quantum nature of the defect is simulated properly and only long-ranged interactions do affect the defect potential in neighboring cells. If the long-range potential possess a Fourier-transformation, e.g. as shown here for  $V_{\text{el-st}}^{\text{lr}}$  (equation (3)) and  $V_{\text{el-ph}}^{\text{lr}}$  (equation (7)), then, it is possible to correct the biased energies *a posteriori*. For this, to have simple evaluable sums and integrals Freysoldt *et al* suggest to model  $\rho_d$  with a simple isotropic function  $\rho_m$ , such as an exponential or a Gaussian (the fitting of  $\rho_d$  by  $\rho_m$  is demonstrated in appendix A). The actual detailed excess-charge distribution is not necessary to know and would change the correction only negligibly. (As Freysoldt *et al* in their original paper note it is not even important to imitate the proper localization of  $\rho_d$  as long as the distribution is well-localized within the supercell.) With this, it is possible to evaluate the lattice sum of the long-range potential (i.e. the potential energy due to their periodic arrangement):

$$E_{\text{latt}} = \frac{1}{\Omega} \sum_{\mathbf{G} \neq 0} V^{\text{lr}}(\mathbf{G}) q_m(\mathbf{G}) \quad (\text{C.1})$$

(for the detailed nomenclature see main text), where  $V(\mathbf{G})$  is the Fourier-transform of the long-range potential, and the sum runs over all reciprocal lattice vectors  $|\mathbf{G}| < G_{\text{cut}}$ . The cut-off  $G_{\text{cut}}$  has to be chosen carefully to ensure convergence of the sum. Equation (C.1) is the artificial energy, which has to be removed from the regarded energy (e.g. the polaron binding energy or level). What is missing is the long-range energy of the isolated defect. This is easily calculated by:

$$E_{\text{iso}} = \frac{1}{(2\pi)^3} \int V(\mathbf{k}) q_d(\mathbf{k}) d\mathbf{k} \quad (\text{C.2})$$

and the total correction is given by  $E_{\text{corr}} = E_{\text{latt}} - E_{\text{iso}}$ . To obtain the desired energy in its dilute  $E_{\infty}$  limit the correction  $E_{\text{corr}}(\Omega)$  has to be removed from the energy  $E(\Omega)$  calculated in the supercell of size  $\Omega$ :

$$E_{\infty} = E(\Omega) - E_{\text{corr}}(\Omega) + q\Delta V. \quad (\text{C.3})$$

The last term  $q\Delta V$  is the so-called alignment term and has to be considered for the following reasons: first, usually  $E(\Omega)$  is calculated with respect to a reference system, often the pristine bulk system. Due to defect or the charge there might be difference in the potentials for the defect system and the pristine system even far away

from the defect center. This difference can be obtained by aligning the electrostatic potentials (or Hartree potentials). Second, the absolute position of the long-range potential calculated from  $\rho_m$  might not be equal to the one from the original  $\rho_d$ . This difference must be aligned, too. Hence, in general the term  $q\Delta V$  should include these two contributions.

## ORCID iDs

Sebastian Kokott  <https://orcid.org/0000-0003-1066-6909>

## References

- [1] Henderson M A 2011 A surface science perspective on photocatalysis *Surf. Sci. Rep.* **66** 185–297
- [2] Dohnálek Z, Lyubintsev I and Rousseau R 2010 Thermally-driven processes on rutile  $\text{TiO}_2(110)$ - $(1 \times 1)$ : a direct view at the atomic scale *Prog. Surf. Sci.* **85** 161–205
- [3] Zhu X-Y and Podzorov V 2015 Charge carriers in hybrid organic–inorganic lead halide perovskites might be protected as large polarons *J. Phys. Chem. Lett.* **6** 4758–61
- [4] Yang S, Brant A T, Giles N C and Halliburton L E 2013 Intrinsic small polarons in rutile  $\text{TiO}_2$  *Phys. Rev. B* **87** 125201
- [5] Sezen H et al 2015 Evidence for photogenerated intermediate hole polarons in ZnO *Nat. Commun.* **6** 6901
- [6] Setvin M, Franchini C, Hao X, Schmid M, Janotti A, Kaltak M, Van de Walle C G, Kresse G and Diebold U 2014 Direct view at excess electrons in  $\text{TiO}_2$  rutile and anatase *Phys. Rev. Lett.* **113** 086402
- [7] Fröhlich H 1954 Electrons in lattice fields *Adv. Phys.* **3** 325–61
- [8] Holstein T 1959 Studies of polaron motion: II. The small polaron *Ann. Phys., NY* **8** 343–89
- [9] Sadigh B, Erhart P and Åberg D 2015 Variational polaron self-interaction-corrected total-energy functional for charge excitations in insulators *Phys. Rev. B* **92** 075202
- [10] Makov G and Payne M C 1995 Periodic boundary conditions in *ab initio* calculations *Phys. Rev. B* **51** 4014–22
- [11] Scheffler M, Vigneron J P and Bachelet G B 1985 Total-energy gradients and lattice distortions at point defects in semiconductors *Phys. Rev. B* **31** 6541
- [12] Freysoldt C, Neugebauer J and Van de Walle C G 2009 Fully *ab initio* finite-size corrections for charged-defect supercell calculations *Phys. Rev. Lett.* **102** 016402
- [13] Devreese J T 2016 Fröhlich polarons. Lecture course including detailed theoretical derivations arXiv:1611.06122
- [14] Verdi C and Giustino F 2015 Fröhlich electron-phonon vertex from first principles *Phys. Rev. Lett.* **115** 176401
- [15] Fock H, Kramer B and Büttner H 1975 Polarons and effective electron-hole interaction in anisotropic polar crystals *Phys. Status Solidi b* **67** 199–206
- [16] Pekar S I 1946 Autolocalization of the electron in an inertially polarizable dielectric medium *Zh. Eksp. Teor. Fiz.* **16** 335
- [17] Freysoldt C, Neugebauer J and Van de Walle C G 2011 Electrostatic interactions between charged defects in supercells *Phys. Status Solidi b* **248** 1067–76
- [18] Heyd J, Scuseria G E and Ernzerhof M 2003 Hybrid functionals based on a screened Coulomb potential *J. Chem. Phys.* **118** 8207–15
- [19] Heyd J, Scuseria G E and Ernzerhof M 2006 Erratum: hybrid functionals based on a screened Coulomb potential *J. Chem. Phys.* **124** 219906
- [20] Atalla V, Yoon M, Caruso F, Rinke P and Scheffler M 2013 Hybrid density functional theory meets quasiparticle calculations: a consistent electronic structure approach *Phys. Rev. B* **88** 165122
- [21] Atalla V, Zhang I Y, Hofmann O T, Ren X, Rinke P and Scheffler M 2016 Enforcing the linear behavior of the total energy with hybrid functionals: implications for charge transfer, interaction energies, and the random-phase approximation *Phys. Rev. B* **94** 035140
- [22] Lany S 2011 Predicting polaronic defect states by means of generalized Koopmans density functional calculations *Phys. Status Solidi b* **248** 1052–60
- [23] Skone J H, Govoni M and Galli G 2014 Self-consistent hybrid functional for condensed systems *Phys. Rev. B* **89** 195112
- [24] Dauth M, Caruso F, Kümmel S and Rinke P 2016 Piecewise linearity in the GW approximation for accurate quasiparticle energy predictions *Phys. Rev. B* **93** 121115
- [25] Refaely-Abramson S, Baer R and Kronik L 2011 Fundamental and excitation gaps in molecules of relevance for organic photovoltaics from an optimally tuned range-separated hybrid functional *Phys. Rev. B* **84** 075144
- [26] Stein T, Eisenberg H, Kronik L and Baer R 2010 Fundamental gaps in finite systems from eigenvalues of a generalized Kohn–Sham method *Phys. Rev. Lett.* **105** 266802
- [27] Perdew J P, Parr R G, Levy M and Balduz J L 1982 Density-functional theory for fractional particle number: derivative discontinuities of the energy *Phys. Rev. Lett.* **49** 1691–4
- [28] Perdew J P et al 2017 Understanding band gaps of solids in generalized Kohn–Sham theory *Proc. Natl Acad. Sci.* **114** 2801–6
- [29] Lany S and Zunger A 2009 Polaronic hole localization and multiple hole binding of acceptors in oxide wide-gap semiconductors *Phys. Rev. B* **80** 085202
- [30] Zawadzki P, Jacobsen K W and Rossmeisl J 2011 Electronic hole localization in rutile and anatase  $\text{TiO}_2$  self-interaction correction in -SCF DFT *Chem. Phys. Lett.* **506** 42–5
- [31] Lemmens L F and Devreese J T 1973 The 1:2:3:4 theorem and the ground state of free polarons *Solid State Commun.* **12** 1067–69
- [32] Levchenko S V, Ren X, Wieferink J, Johanni R, Rinke P, Blum V and Scheffler M 2015 Hybrid functionals for large periodic systems in an all-electron, numeric atom-centered basis framework *Comput. Phys. Commun.* **192** 60–9
- [33] Blum V, Gehrke R, Hanke F, Havu P, Havu V, Ren X, Reuter K and Scheffler M 2009 *Ab initio* molecular simulations with numeric atom-centered orbitals *Comput. Phys. Commun.* **180** 2196
- [34] Havu V, Blum V, Havu P and Scheffler M 2009 Efficient  $o(n)$  integration for all-electron electronic structure calculation using numeric basis functions *J. Comput. Phys.* **228** 8367
- [35] Ren X, Rinke P, Blum V, Wieferink J, Tkatchenko A, Andrea S, Reuter K, Blum V and Scheffler M 2012 Resolution-of-identity approach to Hartree–Fock, hybrid density functionals, RPA, MP2, and GW with numeric atom-centered orbital basis functions *New J. Phys.* **14** 053020

- [36] Deskins N A and Dupuis M 2007 Electron transport via polaron hopping in bulk TiO<sub>2</sub>: a density functional theory characterization *Phys. Rev. B* **75** 195212
- [37] Spreafico C and VandeVondele J 2014 The nature of excess electrons in anatase and rutile from hybrid DFT and RPA *Phys. Chem. Chem. Phys.* **16** 26144–52
- [38] Janotti A, Franchini C, Varley J B, Kresse G and Van de Walle C G 2013 Dual behavior of excess electrons in rutile TiO<sub>2</sub> *Phys. Status Solidi* **7** 199–203
- [39] Moser S et al 2013 Tunable polaronic conduction in anatase TiO<sub>2</sub> *Phys. Rev. Lett.* **110** 196403
- [40] Verdi C, Caruso F and Giustino F 2017 Origin of the crossover from polarons to Fermi liquids in transition metal oxides *Nat. Commun.* **8** 15769
- [41] Feynman R P 1955 Slow electrons in a polar crystal *Phys. Rev.* **97** 660–5
- [42] Allcock G R 1956 On the polaron rest energy and effective mass *Adv. Phys.* **5** 412–51
- [43] Madelung O 2004 *Semiconductors: Data Handbook* (Berlin: Springer) (<https://doi.org/10.1007/978-3-642-18865-7>)
- [44] Pascual J, Camassel J and Mathieu H 1978 Fine structure in the intrinsic absorption edge of TiO<sub>2</sub> *Phys. Rev. B* **18** 5606–14
- [45] Abazović N D, Čomor M I, Dramićanin M D, Jovanović D J, Ahrenkiel S P and Nedeljković J M 2006 Photoluminescence of anatase and rutile TiO<sub>2</sub> particles *J. Phys. Chem. B* **110** 25366–70
- [46] Hedin L 1965 New method for calculating the one-particle Green's Function with application to the electron-gas Problem *Phys. Rev.* **139** A796
- [47] Rinke P, Qteish A, Neugebauer J, Freysoldt C and Scheffler M 2005 Combining GW calculations with exact-exchange density-functional theory: an analysis of valence-band photoemission for compound semiconductors *New J. Phys.* **7** 126
- [48] Rinke P, Schleife A, Kioupakis E, Janotti A, Rödl C, Bechstedt F, Scheffler M and Van de Walle C G 2012 First-principles optical spectra for F centers in MgO *Phys. Rev. Lett.* **108** 126404
- [49] Luttinger J M and Kohn W 1955 Motion of electrons and holes in perturbed periodic fields *Phys. Rev.* **97** 869–83
- [50] Rachko Z A and Valbis J A 1979 Luminescence of free and relaxed excitons in MgO *Phys. Status Solidi b* **93** 161–6